Published in final edited form as:
Toxicol Lett. 2012 May 20; 211(1): 29–38. doi:10.1016/j.toxlet.2012.02.017.

Pharmacologic ER Stress Induces Non-alcoholic Steatohepatitis in an Animal Model

Jin-Sook Lee[1,#], **Ze Zheng**[1,#], **Roberto Mendez**[1], **Seung-Wook Ha**[3], **Youming Xie**[3], and **Kezhong Zhang**[1,2,3,*]

[1]Center for Molecular Medicine and Genetics, The Wayne State University School of Medicine, Detroit, MI 48201, USA

[2]Department of Immunology and Microbiology, The Wayne State University School of Medicine, Detroit, MI 48201, USA

[3]Karmanos Cancer Institute, The Wayne State University School of Medicine, Detroit, MI 48201, USA

Abstract

Endoplasmic reticulum (ER) stress refers to a condition of accumulation of unfolded or misfolded proteins in the ER lumen, which is known to activate an intracellular stress signaling termed Unfolded Protein Response (UPR). A number of pharmacologic reagents or pathophysiologic stimuli can induce ER stress and activation of the UPR signaling, leading to alteration of cell physiology that is associated with the initiation and progression of a variety of diseases. Non-alcoholic steatohepatitis (NASH), characterized by hepatic steatosis and inflammation, has been considered the precursor or the hepatic manifestation of metabolic disease. In this study, we delineated the toxic effect and molecular basis by which pharmacologic ER stress, induced by a bacterial nucleoside antibiotic tunicamycin (TM), promotes NASH in an animal model. Mice of C57BL/6J strain background were challenged with pharmacologic ER stress by intraperitoneal injection of TM. Upon TM injection, mice exhibited a quick NASH state characterized by hepatic steatosis and inflammation. An increase in hepatic triglycerides (TG) and a decrease in plasma lipids, including plasma TG, plasma cholesterol, high-density lipoprotein (HDL), and low-density lipoprotein (LDL), were observed in the TM-treated mice. In response to TM challenge, cleavage of sterol responsive binding protein (SREBP)-1a and SREBP-1c, the key *trans*-activators for lipid and sterol biosynthesis, was dramatically increased in the liver. Consistent with the hepatic steatosis phenotype, expression of some key regulators and enzymes in *de novo* lipogenesis and lipid droplet formation was up-regulated, while expression of those involved in lipolysis and fatty acid oxidation was down-regulated in the liver of mice challenged with TM. Moreover, TM treatment significantly increased phosphorylation of NF-κB inhibitors (IκB), leading to the activation of NF-κB-mediated inflammatory pathway in the liver. Our study not only confirmed that pharmacologic ER stress is a strong “hit” that triggers NASH, but also demonstrated crucial molecular links between ER stress, lipid metabolism, and inflammation in the liver *in vivo*.

*Correspondence to: Kezhong Zhang, Ph.D., Center for Molecular Medicine and Genetics, Wayne State University School of Medicine, 540 E. Canfield Avenue, Detroit, MI 48201, USA. Tel: 313-577-2669; FAX: 313-577-5218; kzhang@med.wayne.edu.
#J-S L and ZZ contributed equally to this work

Keywords

ER Stress; Non-alcoholic Steatohepatitis; Tunicamycin; Lipid Metabolism; Hepatic Inflammation

1. Introduction

In eukaryotes, ER is an intracellular organelle responsible for folding of membrane and secreted proteins, synthesis of lipids and sterols, and storage of free calcium (Gething and Sambrook, 1992; Schroder and Kaufman, 2005). A number of pharmacologic and pathophysiological stimuli, such as calcium depletion, altered protein glycosylation, oxidative stress, DNA damage, viral infection, genetic mutations, and energy fluctuation, can impose stress on the ER, interrupting protein folding process. The ER maintains a high-quality control system to ensure that only the correctly-folded proteins are transported out of ER. The unfolded or misfolded proteins are retained in the ER and eventually are refolded or degraded. As a consequence of the stimuli described above, unfolded or misfolded proteins can accumulate in the ER lumen – a condition referred to "ER stress". To ensure the fidelity of protein folding and to handle the accumulation of unfolded or misfolded proteins, the ER has evolved a group of signal transduction pathways collectively termed "Unfolded Protein Response (UPR)" to alter transcriptional and translational programs (Ron and Walter, 2007; Schroder and Kaufman, 2005). The combined effect of the UPR activation is to reprogram the cell to recover from or adapt to ER stress. However, if the attempt to recover from ER stress fails or the ER stress gets prolonged, the UPR will induce cell death programs to eliminate the stressed cells (Zhang and Kaufman, 2008).

Tunicamycin (TM) is a bacterial nucleoside antibiotic that can block N-linked glycoproteins and cause accumulation of unfolded or misfolded proteins in the ER (King and Tabiowo, 1981). TM has been routinely used to induce pharmacologic ER stress and activation of the UPR. Recent research demonstrated that intraperitoneal injection of TM into mice can efficiently induce ER stress in the liver *in vivo* (Marciniak, et al., 2004; Zhang, et al., 2006). The TM-challenged animal model has been used as an experimental tool to study the effect and mechanism by which acute/ pharmacologic ER stress modulates liver metabolism, particularly lipid metabolism (Rutkowski, et al., 2008; Yamamoto, et al., 2010; Zhang, et al., 2011b).

Nonalcoholic steatohepatitis (NASH), characterized by hepatic steatosis and inflammation, is considered the hepatic precursor or hepatic manifestation of metabolic disorders including visceral obesity, diabetes mellitus, dyslipidemia, and hypertension (Brunt, 2001; Papandreou, et al., 2007; Wieckowska, et al., 2007). In the pathogenesis of NASH, hepatic lipid accumulation results from an imbalance between lipid synthesis, storage, oxidation, and/or secretion, and eventually triggers hepatic inflammation and injury (Musso, et al., 2009; Postic and Girard, 2008). The progression of NASH is currently explained by a "two-hit" working model (Day and James, 1998). According to this model, steatosis represents the "first hit," which increases the vulnerability of the liver to various "second hits" induced by endotoxin, saturated fatty acids, inflammatory cytokines, or other liver injuries. The "second hits" in turn lead to hepatic inflammation, fibrosis, and cellular death, the key features of NASH (Wanless and Lentz, 1990). Notably, recent work suggested that endoplasmic reticulum (ER) stress may represent an intrinsic second hit that triggers NASH in the steatotic liver (Wang, et al., 2006; Wei, et al., 2009; Wei, et al., 2006).

In this study, we utilized a TM-challenged mouse model to evaluate pharmacological ER stress as a "hit" to induce non-alcoholic fatty liver disease (NAFLD) phenotype. Our study demonstrated that TM can induce a quick NASH state characterized by hepatic steatosis and

inflammation. TM challenge led to dramatic activation of sterol responsive binding protein (SREBP) 1a and SREBP1c, the key regulators of *de novo* lipogenesis, and activation of NF-κB, a key inflammatory mediator, in the liver. Our study not only confirmed NAFLD phenotype triggered by pharmacological ER stress, but also provided important insights into the regulation of hepatic lipid metabolism and inflammation by ER stress.

2. Materials and Methods

2.1. Materials

Chemicals were purchased from Sigma unless indicated otherwise. Synthetic oligonucleotides were purchased from Integrated DNA Technologies, Inc. (Coralville, IA). Antibodies against SREBP-1c, SREBP-1a, and SREBP2 were from Thermo Scientific (Rockford, IL), Santa Cruz Biotechnologies, Inc (Santa Cruz, CA), and Abcam (Cambridge, MA), respectively. Antibodies against phosphorylated IκB, total IκB, phosphorylated JNK, and total JNK were purchased from Cell Signaling Technologies (Danvers, MA). Antibody against GAPDH was purchased from Sigma (St. Louis, MO). Kits for measuring triglycerides were purchased from BioAssay System, Inc (Hayward, CA). The ELISA kits for measuring mouse TNFα and IL6 were from Biolegend (San Diego, CA). The ELISA kit for measuring mouse serum amyloid component P (SAP) was from Immunology Consultants Laboratory, Inc (Portland, OR).

2.2. Mouse experiments

The wild-type mice on a C57Bl/6J background at 3-months of age were injected intraperitoneally with TM (2μg/gram body weight) or vehicle control (150 μM dextrose). At 8 or 30 hours after TM injection, liver tissue and blood samples were collected for Oil-red O staining, histological analysis, lipid profiling, Western blot analysis, and quantitative real-time PCR analysis. All the animal experiments were approved by the Wayne State University IACUC committee and carried out under the institutional guidelines for ethical animal use.

2.3. Measurement of mouse lipid contents

To determine hepatic TG levels, approximately 100 mg mouse liver tissue was homogenized in PBS followed by centrifugation. The supernatant was mixed with 10% Triton-100 in PBS for TG measurement using a commercial kit (BioAssay Systems, Hayward, CA). Levels of plasma lipids in the mice were determined enzymatically using commercial kits (Roche Diagnostics Corporation). Approximately 120 μl of mouse blood plasma was collected and subjected to analyses using commercial kits for total cholesterol, HDL, and Triglyceride (Allain, et al., 1974; Stein EA, 1994). Levels of plasma LDL were calculated based on the formula: LDL= total cholesterol-HDL-(triglycerides/5).

2.4. Oil-red O staining

Frozen liver tissue sections were stained with Oil-red O for lipid contents according to standard protocol. Briefly, frozen liver tissue sections of 8-microns were air-dried, and then fixed in formalin. The fixed sections were rinsed in 60% isopropanol followed by staining with freshly prepared Oil-red O solution for 15 min. After Oil-red O staining, liver sections were rinsed in 60% isopropanol followed by washing with water before subjected to microscope analysis.

2.5. Histological scoring for NASH activities

Paraffin-embedded liver tissue sections (5-μm) from mice after TM challenge were subjected to hematoxylin and eosin (H&E) staining or Sirius-red staining. The histological

analysis of H&E-stained or Sirius-red-stained tissue sections for liver inflammation and fibrosis was as described previously (Brunt, et al., 1999; Zheng, et al., 2011). Each section was examined by a specialist who was blinded to the sample information. Hepatic steatosis, hepatocyte ballooning, lobular and portal inflammation, Mallory bodies, and fibrosis were examined and scored according to the modified Brunt scoring system for for NAFLD (Brunt, 2001; Brunt, et al., 1999; Kleiner, et al., 2005). The grade scores were calculated based on the scores of steatosis, hepatocyte ballooning, lobular and portal inflammation, and Mallory bodies. The stage scores were based on the liver fibrosis. The 0-3 grading includes: 0, none; 1, mild; 2, moderate; and 3, severe. The fibrosis stages were determined based on the 0-4 stage system: 0, none; 1, zone 3 perisinusoidal fibrosis; 2, zone 3 perisinusoidal fibrosis plus portal fibrosis; 3, perisinusoidal fibrosis, portal fibrosis, plus bridging fibrosis; and 4, cirrhosis.

2.6. Metabolic Labeling for measuring de novo lip lipogenesis

For measuring *de novo* lipogenesis, Huh7 cells were incubated with 1.0 μCi of [1-^{14}C] acetic acid (from Perkin Elmer) for 6 or 12 hours in the presence or absence of TM (20μg/ml). Hepatocytes were washed twice with PBS at 37°C and cellular lipids were extracted as previously described (Bligh and Dyer, 1959). The rates of hepatic de novo lipogenesis are represented by [1-^{14}C] acetic acid incorporation into total lipids after normalization to cell numbers.

2.7. Western Blot Analysis

To determine protein levels of SREBP1a, SREBP-1c, SREBP2, phosphorylated IκB, total IκB, phosphorylated JNK, total JNK, or GAPDH, total cell lysates were prepared from mouse liver tissue using NP-40 lysis buffer as previously described (Laing, et al., 2010). Denatured proteins were separated by SDS-PAGE on 10% Tris-glycine polyacrylamide gels and transferred to a 0.45-mm PVDF membrane (GE Healthcare). Membrane-bound antibodies were detected by an enhanced chemiluminescence detection reagent (GE Healthcare).

2.8. Huh7 cell culture and treatment with TM

Huh7 cells were cultured in DMEM supplemented with 2 mM L-glutamine, 1 mM sodium pyruvate, and 10% fetal bovine serum (FBS) at 37 °C and 5% CO_2. Huh7 cells at 70% confluency were treated with TM (5, 10, and 20 μg/ml) or vehicle PBS for 6, 12, and 24 hours. Total RNAs were extracted from the Huh7 cells after the treatment for quantitative real-time RT-PCR analysis.

2.9. Quantitative real-time RT-PCR analysis

For real-time PCR analysis, the reaction mixture containing cDNA template, primers, and SYBR Green PCR Master Mix (Applied Biosystems) was run in a 7500 Fast Real-time PCR System (Applied Biosystems, Carlsbad, CA). The sequences of real-time PCR primers used in this study are shown in Supplemental information S4. Fold changes of mRNA levels were determined after normalization to internal control β-actin RNA levels. To confirm the gene expression analysis using β-actin as an internal control, we performed quantitative real-time RT-PCR analysis using two other endogenous internal controls, Gapdh and Hprt1, which is reported to provide accurate measurements of gene expression (Vandesompele, et al., 2002). For the quantitative real-time PCR using 2 internal controls, normalization factors were calculated as previously described (Walker, et al., 2009). The normalization factors were derived from the geometric mean of the C_T values of the two controls. RQ values were calculated by the comparative C_T method.

2.10. Statistics

Experimental results are shown as mean ± SEM (for variation between animals or experiments). The differences among means of the comparison between multiple (more than 2) groups were analyzed by one-way analysis of variance (ANOVA) followed by post hoc comparisons of group means with the Tukey-Kramer test. The mean values for biochemical data from 2 experimental groups were compared by a paired or unpaired, 2-tailed Student's *t* test. All data are expressed as the mean ± SEM. Differences with $p < 0.05$ were considered statistically significant.

3. Results

3.1. TM challenge induces a quick NASH state in the liver

TM has been proven an efficient pharmacological tool that induces acute ER stress in the liver *in vivo* (Marciniak, et al., 2004). To study the effect of pharmacological ER stress in liver pathophysiology, we challenged mice with TM through intraperitoneal (IP) injection. After 8 and 30 hours of TM challenge, mouse liver tissue and blood plasma samples were collected for histological analysis, lipid profiling, and gene expression analysis. Through these analyses, we confirmed that levels of the spliced X-box binding protein 1 (Xbp1) mRNA, a potent UPR trans-activator and a target of ER stress sensor IRE1α (Ron and Walter, 2007; Schroder and Kaufman, 2005), were significantly increased at 8 hours after TM injection (Figure 1A). At 30 hours after TM treatment, the levels of spliced Xbp1 mRNA were reduced, compared to that at 8 hours after the challenge, suggesting an adaptation of the liver cells to ER stress at the late phase of TM treatment. Similarly, the expression of ER stress-induced pro-apoptotic factor GADD153/CHOP and ER-associated degradation (ERAD) regulator EDEM1 exhibited the same pattern of increase at 8 hours followed by reduction at 30 hours due to stress adaptation after TM challenge (Figure 1A). This result confirmed that the injection of TM efficiently induced ER stress response in the liver.

Next, we asked whether acute ER stress induced by TM can cause any stage of NAFLD in mice. We first examined lipid profiles in the liver tissues and blood plasma of mice challenged with TM. Hepatic lipid droplets were detected in the liver of mice challenged with TM for 8 hours (Figure 1B). At 30 hours after TM challenge, lipid droplet accumulation in the liver was significantly increased. The TM-induced hepatic lipid accumulation was further confirmed by the quantitative analysis of hepatic triglycerides (TG) (Figure 1C). Along with the hepatic steatosis phenotype, production of plasma lipid species, including plasma TG, total plasma cholesterol (TC), high-density lipoprotein (HDL), and low-density lipoprotein (LDL), was progressively reduced upon TM challenge (Figure 1D). These results indicated a prominent hepatic steatosis and decreased production of plasma lipids caused by acute ER stress, TM challenge.

We then performed histological analyses with liver tissue sections from mice challenged with TM or vehicle control. Analyses of hematoxylin & eosin (H&E) staining of liver cellular structure and Sirius-red staining of collagen deposition indicated that hepatic steatosis and lobular inflammation occurred in the liver after 8 hours of TM treatment (Figure 2A-B). At 30 hours after TM challenge, increased hepatic steatosis, lobular and portal inflammation, as well as slight fibrosis were detected in the liver (Figure 2A-B). However, hepatocyte ballooning and Mallory bodies, the features of advanced NAFLD, were not detected in TM-induced NASH animal model. In summary, our data suggested that TM challenge can induce a quick animal model of NASH characterized by hepatic steatosis and inflammation.

3.2. TM dramatically induces cleavage of SREBP1a and SREBP1c in the liver

Induction of hepatic steatosis and inflammation by TM in animals provides a valuable *in vivo* model system for investigating regulation of hepatic lipid metabolism and inflammatory response by pharmacological ER stress. To determine effects of pharmacological ER stress on hepatic lipid metabolism, we examined activation of major SREBP isoforms SREBP1a, SREBP1c, and SREBP2, the key transcriptional regulators of *de novo* lipogenesis (Horton, et al., 2002a), in the liver of mice exposed to TM or vehicle control. SREBP1a is a potent activator of all SREBP-responsive genes, including those that mediate the synthesis of cholesterol, fatty acid (FA), and TG, while SREBP-1c and SREBP2 preferentially enhance transcription of genes required for synthesis of FA and cholesterol, respectively. Activation of SREBPs is indicated by cleavage of SREBP proteins, a process that can be induced by metabolic conditions, such as insulin signal and cholesterol or sterol deprivation (Horton, et al., 2002a). Surprisingly, upon TM challenge, a dramatic increase in levels of cleaved SREBP1a and SREBP1c proteins was detected in the liver tissues (Figure 3A-B). Indeed, a majority of the SREBP1a precursors and all of SREBP1c precursors were diminished along with the accumulation of the cleaved/mature forms of SREBP1a and SREBP1c in the TM-challenged liver. However, TM has little effect on activation of SREBP2 (Supplemental figure 1). These results suggested that TM challenge may up-regulate *de novo* lipogenesis through activation of SREBP1a and SREBP1c in the liver.

3.3. TM challenge up-regulates expression of genes involved in lipogenesis but down-regulates expression of genes involved in lipolysis and FA oxidation in the liver

Hepatic lipid homeostasis is maintained through multiple lipid-associated pathways, such as fatty acids uptake, *de novo* lipogenesis, lipolysis, FA oxidation, lipid transport and deposition (Musso, et al., 2009; Postic and Girard, 2008). Hepatic steatosis may develop as a consequence of dysregulation of one or multiple lipid-associated pathways. To gain further insights into the hepatic steatosis induced by TM, we performed pathway-specific quantitative real-time RT-PCR analysis with liver tissues from mice treated with TM or vehicle control. Through this analysis, we identified that expression of genes encoding some of the key *trans*-activators and enzymes in *de novo* lipogenesis and lipid droplet production was increased in the liver of mice after TM challenge (Figure 4A-B). These regulators or enzymes include peroxisome proliferator-activated receptor gamma coactivator-1 (PGC1) α, PGC1β, diacylglycerol O-acyltransferase (DGAT) 1, DGAT2, adipose differentiation-related protein (ADRP), fat-inducing transcript (FIT) 2, and fat specific protein 27 (FSP27). Similar to the ER stress-responsive genes (Figure 1A), the expression of these lipogenic genes exhibited a pattern of increase at 8 hours following by adaptation-induced reduction at 30 hours after TM challenge (Figure 4A-B). Moreover, we found that expression of the genes involved in lipolysis and FA oxidation, two processes that break down TG and FA, respectively, were decreased in the liver of mice after TM challenge (Figure 4C-D). These include the genes encoding apolipoprotein C2 (ApoC2), acyl-Coenzyme A oxidase 1 (Acox1), lipolysis stimulated lipoprotein receptor (LSR), and peroxisome proliferator-activated receptor α (PPARα). To confirm the quantitative gene expression analysis results using β-actin as an internal control, we performed quantitative real-time RT-PCR analysis using two other endogenous internal controls, Gapdh and Hprt1. Use of multiple endogenous internal controls is reported to provide accurate measurements of gene expression (Vandesompele, et al., 2002). The results confirmed the TM-induced expression patterns for the lipogenic genes obtained through the gene expression analysis using β-actin as an internal control (Supplemental figure 2). Together, the TM-induced gene expression profile, in which expression of genes involved in lipogenesis was increased while expression of genes in lipolysis and FA oxidation was decreased, may account for, at least partially, the hepatic steatosis induced by TM.

To determine whether pharmacologic ER stress can directly promote hepatic *de novo* lipogenesis, we performed isotope ([1-^{14}C] acetic acids) labeling experiments with a human hepatoma cell line Huh7, a cell line that maintains key features of hepatocytes and has been used for studying hepatic lipid metabolism (Nakabayashi, et al., 1982). The isotope tracing study showed that the rates of *de novo* lipogenesis, reflected by the amounts of ^{14}C-labeled acetic acids incorporated into total lipids, were significantly increased upon TM treatment for 6 or 12 hours, compared to those in the control cells (Figure 4E-F). This result confirmed that ER stress can directly promote hepatic *de novo* lipogenesis. To gain further insights into the ER stress-induced hepatic *de novo* lipogenesis, we characterized the dose- and time-dependent expression patterns of lipogenic genes induced by TM treatment. Upon TM treatment, expression of fatty acid synthase (Fasn) and Adrp, the SREBP1-target genes in hepatic lipogenesis, was induced by TM in Huh7 cells in dose- and time-dependent manners (Supplemental figure 3A-B). Expression of the lipogenic genes Scd1 and Acc1 was also inducible by TM, although the expression levels of these genes were declined, but remained higher than the basal levels, at the late time point of the treatment (12 hours post treatment) (Supplemental figure 3C-D).

3.4. TM activates the inflammatory pathway mediated through NF-κB, but not JNK, in the liver

Next, we determined the pathway through which TM induces inflammation in the liver. Among the major inflammatory pathways we investigated, activation of NF-κB, indicated by increased phosphoryation of NF-κB inhibitor (I-κB), was significantly increased in the liver of mice challenged with TM (Figure 5A). In comparison, the inflammatory pathway mediated through c-Jun N-terminal kinase (JNK) in the liver was only marginally affected by TM treatment (Figure 5B). Supporting the activation of NF-κB-mediated inflammatory pathway, expression of the genes encoding the pro-inflammatory cytokines tumor necrosis factor α (TNFα) and interleukin (IL)-6, two major pro-inflammatory cytokines in promoting NASH activities, was significantly increased in the TM-challenged liver (Figure 6A). Moreover, expression of the genes encoding major murine acute-phase inflammatory responsive proteins, including serum amyloid component P (SAP) and serum amyloid A3 (SAA3), was also increased in the liver in response to TM challenge (Figure 6B). Examination of serum levels of TNFα, IL6, and SAP proteins in the mice after TM treatment confirmed the effect of TM on promoting the production of pro-inflammatory cytokines and hepatic acute-phase responsive protein, the hall marks of hepatic inflammation and NASH phenotype (Figure 6C-E).

4. Discussion

In this study, we demonstrated the toxic effect of pharmacologic ER stress, induced by TM, in promoting NASH in a quick animal model, and provided important insights into the regulation of hepatic lipid metabolism and inflammation by acute ER stress *in vivo*. Our findings include: (1) ER stress-inducing reagent TM can induce a quick NASH state *in vivo*, which is characterized by hepatic steatosis, inflammation, and decreased plasma lipids; (2) TM challenge leads to dramatic increase in cleavage of SREBP1a and SREBP1c, the key transcriptional regulator of *de novo* lipogenesis, in the liver; (3) TM challenge increases expression of genes involved in lipogenesis and lipid droplet formation, but decreases expression of genes involved in lipolysis and FA oxidation; (4) TM significantly activates NF-κB and expression of genes encoding pro-inflammatory cytokines TNFα and IL6 as well as acute-phase proteins SAP and SAA3 in the liver. Our study suggested that pharmacologic ER stress-inducing reagent TM can cause hepatic steatosis by promoting *de novo* lipogenesis while suppressing lipolysis, FA oxidation, and production of plasma lipids (Supplemental figure 4). Meanwhile, TM can also trigger hepatic inflammation by activating NF-κB and acute-phase response.

Our work implicated that acute ER stress, which can be induced by pharmacological drugs, for example, anti-cancer drug Bortezomib, or liver injuries (Zhang, et al., 2011b), represents a strong "hit" that triggers or exacerbates NASH by promoting hepatic lipid accumulation and inflammation. Hepatic steatosis, characterized by excessive accumulation of TG in hepatocytes, is the result of abnormal lipid metabolism caused by increased lipid delivery to the liver, increased *de novo* lipogenesis, reduced FA oxidation, reduced lipolysis, and/or decreased lipid secretion (Musso, et al., 2009; Postic and Girard, 2008). Recent research suggests that ER stress response plays important roles in regulating expression of lipogenic factors, secretion of apolipoproteins, lipid accumulation, and lipotoxicity (Feng, et al., 2003; Lee, et al., 2008; Lee, 2012; Oyadomari, et al., 2008; Rutkowski, et al., 2008; Wei, et al., 2006; Yamamoto, et al., 2010; Zhang, et al., 2012; Zhang, et al., 2011b). In this study, we revealed that pharmacological ER stress induced by TM is a strong inducer of *de novo* lipogenesis, but a suppressor of FA oxidation and lipolysis in the liver. Of particular interest is that TM challenge can lead to a dramatic conversion of the precursors of SREBP1a and SREBP1c into their mature forms in the liver *in vivo* (Figure 3). It has been reported that ER stress-inducing reagents, homocystein and thapsigargin, can induce SREBP cleavage in cultured cells (Bobrovnikova-Marjon, et al., 2008; Colgan, et al., 2007; Lee and Ye, 2004; Werstuck, et al., 2001; Woo, et al., 2005). The *in vitro* studies demonstrated that ER stress-induced SREBP activation relies on the UPR pathway through PERK/eIF2α and is suppressed by over-expression of ER chaperone BiP/GRP78 (Bobrovnikova-Marjon, et al.; 2008, Werstuck, et al., 2001). Because the SREBP/SCAP "anchor" protein Insig1 is a short-lived protein, PERK-mediated translational inhibition results in a rapid depletion of Insig1, leading to activation of SREBP under ER stress (Bobrovnikova-Marjon, et al., 2008; Lee and Ye, 2004). With the animal model, we showed here that pharmacological ER stress induced by TM leads to accumulation of mature SREBP1a and SREBP1c along with diminished SREBP precursors in the liver. This not only provides the molecular evidence of TM-induced lipogenesis, but also confirms that pharmacological ER stress is a strong inducer of SREBP activation. However, it should be noticed that SREBP2, the SREBP isoform that plays a major role in cholesterol biosynthesis (Horton, et al., 2002a), is only slightly induced by ER stress in the liver (Supplemental figure 1). Although INSIG-SCAP interaction plays a key role in SREBP activation, activation of SREBP1 and SREBP2 can be differentially regulated by certain metabolic stress conditions (Hannah, et al., 2001; Horton, et al., 2002a; Sheng, et al., 1995). For example, in the absence of fatty acids and in the presence of sterols, SCAP is able to carry SREBP-1 proteins, but not SREBP-2, to the Golgi apparatus for the processing (Hannah, et al., 2001). Additionally, the availability of SREBP1 and SREBP2 precursors under ER stress condition may also affect the levels of cleaved SREBP1 or SREBP2 proteins in the liver of mice challenged with TM. Future studies are required to elucidate the apparent independent regulation of SREBP-1 and SREBP-2 processing in the liver under the pharmacologic ER stress condition.

Our study has identified multiple ER stress-inducible lipogenic genes. However, it is important to address that expression of ER stress-inducible lipogenic genes exhibits a pattern of up-regulation at the early time point followed by adaptation or decline at the late time point of ER stress treatment (Figure 1A and Figure 4A-B). It is known that both ER stress response and lipid homeostasis are tightly regulated by feedback-adaption regulatory loop (Horton, et al., 2002a, b; Rutkowski, et al., 2006; Zhang, et al., 2011b). Upon ER stress, the unfolded protein response (UPR), which initiates both adaptive and pro-apoptotic pathways, can selectively allow for stress adaptation (Rutkowski, et al., 2006). Consistent with the stress up-regulation-adaptation model, our data showed that the UPR target genes, including Xbp1, Chop and Edem1 (Figure 1A), and ER stress-inducible lipogenic genes, including Dgat1, Dgat2, Adrp, and Fsp27 (Figure 4A-B), were updated at 8 hours of TM treatment but declined at 30 hours post treatment in the liver. Interestingly, we observed that expression of some of ER stress-inducible lipogenic genes, for example, PGC1α and

PGC1β (Figure 4A), was highly induced at the late time point of TM treatment. How these genes are differentially regulated by ER stress and how they contribute to ER stress-induced hepatic lipogenesis/steatosis are intriguing questions to be investigated in the future.

Another important finding in this work is the activation of NF-kB in the liver by TM challenge. As revealed by Western blot analysis and confirmed by expression of pro-inflammatory cytokine genes, TM is a strong inducer of NF-κB activation in the liver *in vivo* (Figures 5-6). Previous studies with *in vitro* culture cells suggested that ER stress can induce NF-κB activation through a non-canonical signaling pathway independent of IκBα phosphorylation (Deng, et al., 2004; Wu, et al., 2004; Zhang and Kaufman, 2008). Under ER stress, PERK/eIF2α-mediated translational attenuation leads to decreased levels of the short-lived IκBα protein, thereby freeing NF-κB for its activation. Unlike canonical signaling pathways that promote IκBα phosphorylation and degradation, the PERK/eIF2α UPR branch does not increase phosphorylated IκBα levels or affect the stability of the protein (Deng, et al., 2004; Wu, et al., 2004). However, based on our observations, acute ER stress can also induce NF-κB activation through increasing phosphorylation of IκBα in the liver. Therefore, ER stress may represent a superb inducer of NF-κB signaling through both canonical and non-canonical pathways.

In summary, our study provided important information in the toxic effect of pharmacological ER stress in liver pathology and confirmed that ER stress is a strong “hit” that triggers NASH. Moreover, our work has also demonstrated crucial molecular links between acute ER stress, lipid metabolism, and inflammation in the liver *in vivo*. For future study, it is intriguing to determine the detailed mechanisms by which acute ER stress regulates activation of SREBP, NF-κB, as well as other lipogenic and inflammatory regulators in the liver.

Supplementary Material

Refer to Web version on PubMed Central for supplementary material.

Acknowledgments

Portions of this work were supported by American Heart Association Grants 09GRNT2280479 and National Institutes of Health (NIH) grants DK090313 and ES017829 to KZ. RM is a trainee of NIH training grant NIGMS R25GM058905 Initiative for Maximizing Student Development (IMSD) Program.

Abbreviations

ER	endoplasmic reticulum
TM	tunicamycin
NASH	non-alcoholic steatohepatitis
NAFLD	non-alcoholic fatty liver disease
TG	triglycerides
SREBP	sterol responsive binding protein
NF-κB	activation of nuclear factor-kappa B
IκB	NF-κB inhibitor

References

Allain CC, Poon LS, Chan CS, Richmond W, Fu PC. Enzymatic determination of total serum cholesterol. Clinical chemistry. 1974; 20:470–475. [PubMed: 4818200]

Bligh EG, Dyer WJ. A rapid method of total lipid extraction and purification. Canadian journal of biochemistry and physiology. 1959; 37:911–917. [PubMed: 13671378]

Bobrovnikova-Marjon E, Hatzivassiliou G, Grigoriadou C, Romero M, Cavener DR, Thompson CB, Diehl JA. PERK-dependent regulation of lipogenesis during mouse mammary gland development and adipocyte differentiation. Proc Natl Acad Sci U S A. 2008; 105:16314–16319. [PubMed: 18852460]

Brunt EM. Nonalcoholic steatohepatitis: definition and pathology. Seminars in liver disease. 2001; 21:3–16. [PubMed: 11296695]

Brunt EM, Janney CG, Di Bisceglie AM, Neuschwander-Tetri BA, Bacon BR. Nonalcoholic steatohepatitis: a proposal for grading and staging the histological lesions. Am J Gastroenterol. 1999; 94:2467–2474. [PubMed: 10484010]

Colgan SM, Tang D, Werstuck GH, Austin RC. Endoplasmic reticulum stress causes the activation of sterol regulatory element binding protein-2. The international journal of biochemistry & cell biology. 2007; 39:1843–1851.

Day CP, James OF. Steatohepatitis: a tale of two "hits"? Gastroenterology. 1998; 114:842–845. [PubMed: 9547102]

Deng J, Lu PD, Zhang Y, Scheuner D, Kaufman RJ, Sonenberg N, Harding HP, Ron D. Translational repression mediates activation of nuclear factor kappa B by phosphorylated translation initiation factor 2. Mol Cell Biol. 2004; 24:10161–10168. [PubMed: 15542827]

Feng B, Yao PM, Li Y, Devlin CM, Zhang D, Harding HP, Sweeney M, Rong JX, Kuriakose G, Fisher EA, Marks AR, Ron D, Tabas I. The endoplasmic reticulum is the site of cholesterol-induced cytotoxicity in macrophages. Nat Cell Biol. 2003; 5:781–792. [PubMed: 12907943]

Gething MJ, Sambrook J. Protein folding in the cell. Nature. 1992; 355:33–45. [PubMed: 1731198]

Hannah VC, Ou J, Luong A, Goldstein JL, Brown MS. Unsaturated fatty acids down-regulate srebp isoforms 1a and 1c by two mechanisms in HEK-293 cells. J Biol Chem. 2001; 276:4365–4372. [PubMed: 11085986]

Horton JD, Goldstein JL, Brown MS. SREBPs: activators of the complete program of cholesterol and fatty acid synthesis in the liver. J Clin Invest. 2002a; 109:1125–1131. [PubMed: 11994399]

Horton JD, Goldstein JL, Brown MS. SREBPs: transcriptional mediators of lipid homeostasis. Cold Spring Harbor symposia on quantitative biology. 2002b; 67:491–498.

King IA, Tabiowo A. Effect of tunicamycin on epidermal glycoprotein and glycosaminoglycan synthesis in vitro. Biochem J. 1981; 198:331–338. [PubMed: 7326010]

Kleiner DE, Brunt EM, Van Natta M, Behling C, Contos MJ, Cummings OW, Ferrell LD, Liu YC, Torbenson MS, Unalp-Arida A, Yeh M, McCullough AJ, Sanyal AJ. Design and validation of a histological scoring system for nonalcoholic fatty liver disease. Hepatology. 2005; 41:1313–1321. [PubMed: 15915461]

Laing S, Wang G, Briazova T, Zhang C, Wang A, Zheng Z, Gow A, Chen AF, Rajagopalan S, Chen LC, Sun Q, Zhang K. Airborne particulate matter selectively activates endoplasmic reticulum stress response in the lung and liver tissuesAmerican journal of physiology. Cell physiology. 2010; 299:C736–749. [PubMed: 20554909]

Lee AH, Scapa EF, Cohen DE, Glimcher LH. Regulation of hepatic lipogenesis by the transcription factor XBP1. Science. 2008; 320:1492–1496. [PubMed: 18556558]

Lee JS, Mendez R, Heng HH, Yang Z-Q, Zhang K. Pharmacological ER stress promotes hepatic lipogenesis and lipid droplet formation. Am J Translational Res. 2012; 4:102–113.

Lee JN, Ye J. Proteolytic activation of sterol regulatory element-binding protein induced by cellular stress through depletion of Insig-1. J Biol Chem. 2004; 279:45257–45265. [PubMed: 15304479]

Marciniak SJ, Yun CY, Oyadomari S, Novoa I, Zhang Y, Jungreis R, Nagata K, Harding HP, Ron D. CHOP induces death by promoting protein synthesis and oxidation in the stressed endoplasmic reticulum. Genes & development. 2004; 18:3066–3077. [PubMed: 15601821]

Musso G, Gambino R, Cassader M. Recent insights into hepatic lipid metabolism in non-alcoholic fatty liver disease (NAFLD). Progress in lipid research. 2009; 48:1–26. [PubMed: 18824034]

Nakabayashi H, Taketa K, Miyano K, Yamane T, Sato J. Growth of human hepatoma cells lines with differentiated functions in chemically defined medium. Cancer research. 1982; 42:3858–3863. [PubMed: 6286115]

Oyadomari S, Harding HP, Zhang Y, Oyadomari M, Ron D. Dephosphorylation of translation initiation factor 2alpha enhances glucose tolerance and attenuates hepatosteatosis in mice. Cell Metab. 2008; 7:520–532. [PubMed: 18522833]

Papandreou D, Rousso I, Mavromichalis I. Update on non-alcoholic fatty liver disease in children. Clin Nutr. 2007; 26:409–415. [PubMed: 17449148]

Postic C, Girard J. Contribution of de novo fatty acid synthesis to hepatic steatosis and insulin resistance: lessons from genetically engineered mice. J Clin Invest. 2008; 118:829–838. [PubMed: 18317565]

Ron D, Walter P. Signal integration in the endoplasmic reticulum unfolded protein response. Nat Rev Mol Cell Biol. 2007; 8:519–529. [PubMed: 17565364]

Rutkowski DT, Arnold SM, Miller CN, Wu J, Li J, Gunnison KM, Mori K, Sadighi Akha AA, Raden D, Kaufman RJ. Adaptation to ER stress is mediated by differential stabilities of pro-survival and pro-apoptotic mRNAs and proteins. PLoS Biol. 2006; 4:e374. [PubMed: 17090218]

Rutkowski DT, Wu J, Back SH, Callaghan MU, Ferris SP, Iqbal J, Clark R, Miao H, Hassler JR, Fornek J, Katze MG, Hussain MM, Song B, Swathirajan J, Wang J, Yau GD, Kaufman RJ. UPR pathways combine to prevent hepatic steatosis caused by ER stress-mediated suppression of transcriptional master regulators. Developmental cell. 2008; 15:829–840. [PubMed: 19081072]

Schroder M, Kaufman RJ. The Mammalian unfolded protein response. Annu Rev Biochem. 2005; 74:739–789. [PubMed: 15952902]

Sheng Z, Otani H, Brown MS, Goldstein JL. Independent regulation of sterol regulatory element-binding proteins 1 and 2 in hamster liver. Proc Natl Acad Sci U S A. 1995; 92:935–938. [PubMed: 7862668]

Stein, EA.; MG. Lipids, Lipoproteins, and Apolipoproteins. In: Burtis, CA.; AE, editors. Tietz Textbook of Clinical Chemistry. W.B. Saunders Co; Philadelphia: 1994. p. 1002-1093.

Vandesompele J, De Preter K, Pattyn F, Poppe B, Van Roy N, De Paepe A, Speleman F. Accurate normalization of real-time quantitative RT-PCR data by geometric averaging of multiple internal control genes. Genome biology. 2002; 3:RESEARCH0034. [PubMed: 12184808]

Walker CG, Meier S, Mitchell MD, Roche JR, Littlejohn M. Evaluation of real-time PCR endogenous control genes for analysis of gene expression in bovine endometrium. BMC molecular biology. 2009; 10:100. [PubMed: 19878604]

Wang D, Wei Y, Pagliassotti MJ. Saturated fatty acids promote endoplasmic reticulum stress and liver injury in rats with hepatic steatosis. Endocrinology. 2006; 147:943–951. [PubMed: 16269465]

Wanless IR, Lentz JS. Fatty liver hepatitis (steatohepatitis) and obesity: an autopsy study with analysis of risk factors. Hepatology. 1990; 12:1106–1110. [PubMed: 2227807]

Wei Y, Wang D, Gentile CL, Pagliassotti MJ. Reduced endoplasmic reticulum luminal calcium links saturated fatty acid-mediated endoplasmic reticulum stress and cell death in liver cells. Mol Cell Biochem. 2009; 331:31–40. [PubMed: 19444596]

Wei Y, Wang D, Topczewski F, Pagliassotti MJ. Saturated fatty acids induce endoplasmic reticulum stress and apoptosis independently of ceramide in liver cells. American journal of physiology. Endocrinology and metabolism. 2006; 291:E275–281. [PubMed: 16492686]

Werstuck GH, Lentz SR, Dayal S, Hossain GS, Sood SK, Shi YY, Zhou J, Maeda N, Krisans SK, Malinow MR, Austin RC. Homocysteine-induced endoplasmic reticulum stress causes dysregulation of the cholesterol and triglyceride biosynthetic pathways. J Clin Invest. 2001; 107:1263–1273. [PubMed: 11375416]

Wieckowska A, McCullough AJ, Feldstein AE. Noninvasive diagnosis and monitoring of nonalcoholic steatohepatitis: present and future. Hepatology. 2007; 46:582–589. [PubMed: 17661414]

Woo CW, Siow YL, Pierce GN, Choy PC, Minuk GY, Mymin DOK. Hyperhomocysteinemia induces hepatic cholesterol biosynthesis and lipid accumulation via activation of transcription factors.

American journal of physiology. Endocrinology and metabolism. 2005; 288:E1002–1010. [PubMed: 15644462]

Wu S, Tan M, Hu Y, Wang JL, Scheuner D, Kaufman RJ. Ultraviolet light activates NFkappaB through translational inhibition of IkappaBalpha synthesis. J Biol Chem. 2004; 279:34898–34902. [PubMed: 15184376]

Yamamoto K, Takahara K, Oyadomari S, Okada T, Sato T, Harada A, Mori K. Induction of liver steatosis and lipid droplet formation in ATF6alpha-knockout mice burdened with pharmacological endoplasmic reticulum stress. Mol Biol Cell. 2010; 21:2975–2986. [PubMed: 20631254]

Zhang C, Wang G, Zheng Z, Maddipati KR, Zhang X, Dyson G, Williams P, Duncan SA, Kaufman RJ, Zhang K. Endoplasmic reticulum-tethered transcription factor cAMP responsive element-binding protein, hepatocyte specific, regulates hepatic lipogenesis, fatty acid oxidation, and lipolysis upon metabolic stress in mice. Hepatology. 2012; 55:1070–1082. [PubMed: 22095841]

Zhang K, Kaufman RJ. Identification and characterization of endoplasmic reticulum stress-induced apoptosis in vivo. Methods Enzymol. 2008; 442:395–419. [PubMed: 18662581]

Zhang K, Shen X, Wu J, Sakaki K, Saunders T, Rutkowski DT, Back SH, Kaufman RJ. Endoplasmic reticulum stress activates cleavage of CREBH to induce a systemic inflammatory response. Cell. 2006; 124:587–599. [PubMed: 16469704]

Zhang K, Wang S, Malhotra J, Hassler JR, Back SH, Wang G, Chang L, Xu W, Miao H, Leonardi R, Chen YE, Jackowski S, Kaufman RJ. The unfolded protein response transducer IRE1alpha prevents ER stress-induced hepatic steatosis. EMBO J. 2011b; 30:1357–1375. [PubMed: 21407177]

Zheng Z, Zhang C, Zhang K. Measurement of ER stress response and inflammation in the mouse model of nonalcoholic fatty liver disease. Methods Enzymol. 2011; 489:329–348. [PubMed: 21266239]

Highlights

- Pharmacologic ER stress induced by Tunicamycin (TM) induces a quick NASH state *in vivo*;
- TM leads to dramatic increase in cleavage of sterol regulatory element-binding protein in the liver;
- TM up-regulates lipogenic genes, but down-regulates the genes in lipolysis and FA oxidation;
- TM activates NF-κB and expression of genes encoding pro-inflammatory cytokines in the liver.

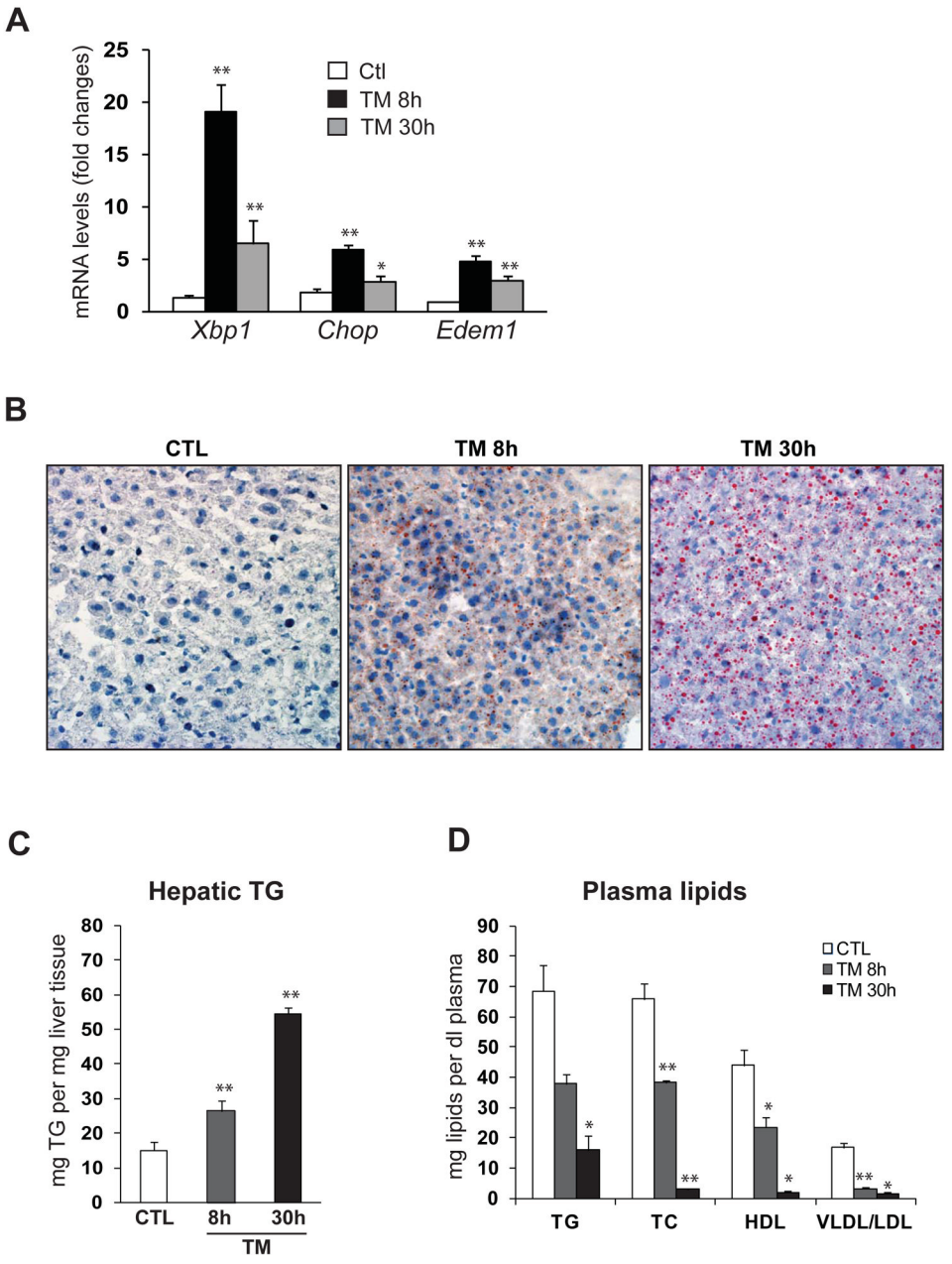

Figure 1. TM challenge alters lipid profiles and causes hepatic steatosis in mice

(A) Quantitative real-time RT-PCR analysis of liver mRNA isolated from mice challenged with TM or vehicle control. Total liver mRNA was isolated at 8 or 30 hours after injection with vehicle or TM (2 μg/gram body weight) for real-time RT-PCR analysis. Expression values were normalized to *β-actin* mRNA levels. Fold changes of mRNA are shown by comparing to one of the control mice. Each bar denotes the mean ± SEM (n=4 mice per group); ** $P<0.01$. Edem1, ER degradation enhancing, mannosidase alpha-like 1. (B) Oil-red O staining of lipid droplets in the livers of the mice challenged with TM or vehicle control (magnification: 200x). (C) Levels of TG in the liver tissues of the mice challenged with TM or vehicle control. (D) Levels of plasma lipids in the mice challenged with TM or vehicle control. TG, triglycerides; TC, total plasma cholesterol; HDL, high-density

lipoproteins; VLDL/ LDL, very low and low density lipoproteins. For C-D, each bar denotes mean ± SEM (n=4 mice per group); * $p<0.05$. ** $p<0.01$.

A

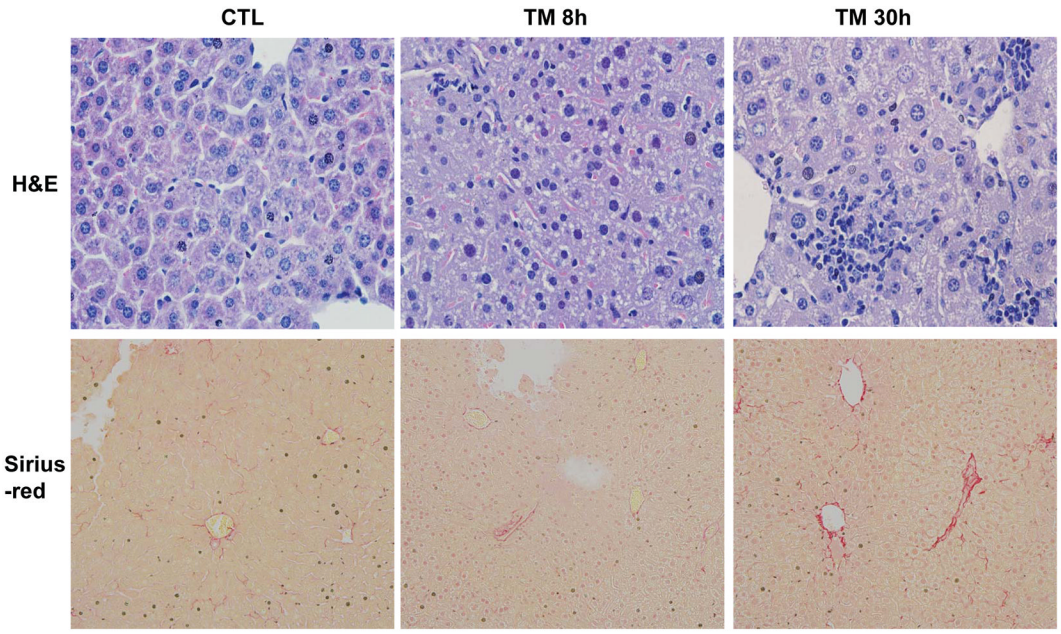

B

NAFLD grading and staging in C57BL/6 mice in the absence or presence of Tm treatment

	Steatosis	Ballooning	Lobular inflammation	Portal inflammation	Mallory bodies	Grade (0-3)	Stage (0-4)
Ctl (3)	0.00 ± 0.00	0.00 ± 0.00	0.33 ± 0.33	0.00 ± 0.00	0.00 ± 0.00	0.00 ± 0.00	1.00 ± 0.58
Tm 8h (3)	1.33 ± 0.33	0.00 ± 0.00	0.67 ± 0.33	0.00 ± 0.00	0.00 ± 0.00	1.67 ± 0.33	0.67 ± 0.33
P -value	0.057	N/A	0.52	N/A	N/A	0.037	0.65
Ctl (3)	0.00 ± 0.00	0.00 ± 0.00	0.33 ± 0.33	0.00 ± 0.00	0.00 ± 0.00	0.00 ± 0.00	1.00 ± 0.58
Tm 30h (6)	1.67 ± 0.33	0.00 ± 0.00	2.00 ± 0.37	0.33 ± 0.21	0.00 ± 0.00	1.83 ± 0.31	0.83 ± 0.40
P -value	0.004	N/A	0.014	0.17	N/A	0.002	0.82

Number of mice examined is given in parentheses. Mean ± SEM values are shown. *P*-values were calculated by Mann-Whitney *U*-test.

Figure 2. TM challenge leads to a quick NASH state in mice

(**A**) Histological examination of liver tissue sections of the mice challenged with TM (2 μg/gram body weight) or vehicle control. Upper panel, hematoxylin eosin (H&E) staining of liver tissue sections; the lower panel, Sirius staining of collagen deposition of liver tissue sections (magnification: 200x). (**B**) Histological scoring for NASH activities in the livers of the mice treated with TM or vehicle control. The Grade scores were calculated based on the scores of steatosis, hepatocyte ballooning, lobular and portal inflammation, and Mallory bodies. The Stage scores were based on the liver fibrosis. Number of mice examined is given in parentheses. Mean ± SEM values are shown. P-values were calculated by Mann-Whitney U-test.

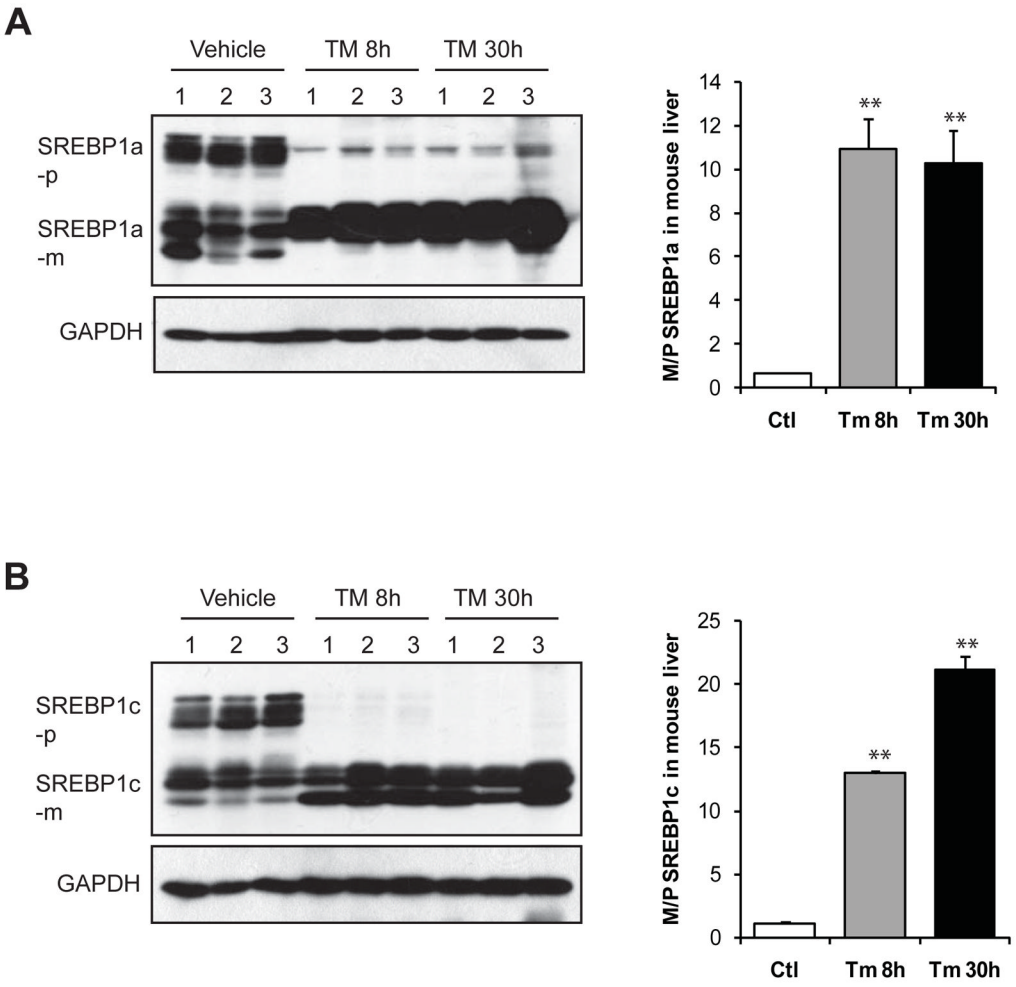

Figure 3. TM challenge significantly increases levels of cleaved/activated forms of SREBP1a and SREBP1c in the liver

Western blot analysis of protein levels of SREBP1a (A) and SREBP1c (B) in the liver tissues from the mice challenged with TM (2 μg/gram body weight) or vehicle control. Levels of GAPDH were included as internal controls. For A-B, the graph beside the images showed the ratios of mature/cleaved SREBP to precursor SREBP in the liver of mice challenged with TM or vehicle. The protein signal intensities shown by Western blot analysis were quantified by NIH imageJ software. Each bar represents the mean ± SEM (n=3 mice per group); ** $p<0.01$. SREBP-p, SREBP precursor; SREBP-m, mature/cleaved SREBP.

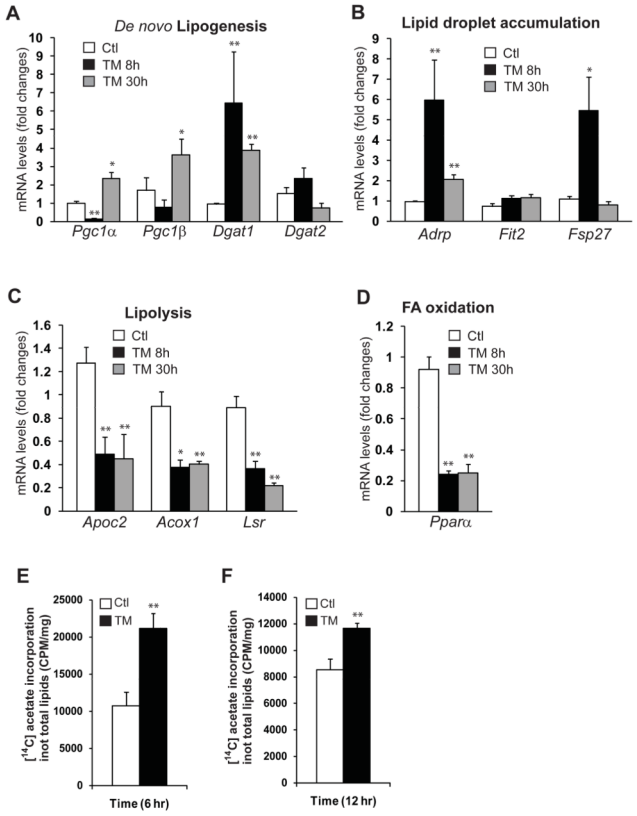

Figure 4. TM challenge up-regulates expression of genes involved in lipogenesis but down-regulates expression of genes involved in lipolysis and FA oxidation

Quantitative real-time RT-PCR analysis of liver mRNAs isolated from the mice challenged with TM (2 μg/gram body weight) or vehicle control, which encode regulators or enzymes in: (A) *de novo* lipogenesis: PGC1α, PGC1β, DGAT1 and DGAT2; (B) lipid droplet production: ADRP, FIT2, and FSP27; (C) lipolysis: ApoC2, Acox1, and LSR; and (D) FA oxidation: PPARα. Expression values were normalized to *β-actin* mRNA levels. Fold changes of mRNA are shown by comparing to one of the control mice. Each bar denotes the mean ± SEM (n=4 mice per group); ** $P<0.01$. (E-F) Isotope tracing analysis of hepatic *de novo lip genesis.* Huh7 cells were incubated with [1-^{14}C] acetic acid for 6 hours (E) or 12 hours (F) in the presence or absence of TM (20μg/ml). The rates of *de novo* lipogenesis were quantified by determining the amounts of [1-^{14}C]-labeled acetic acid incorporated into total cellular lipids after normalization to cell numbers.

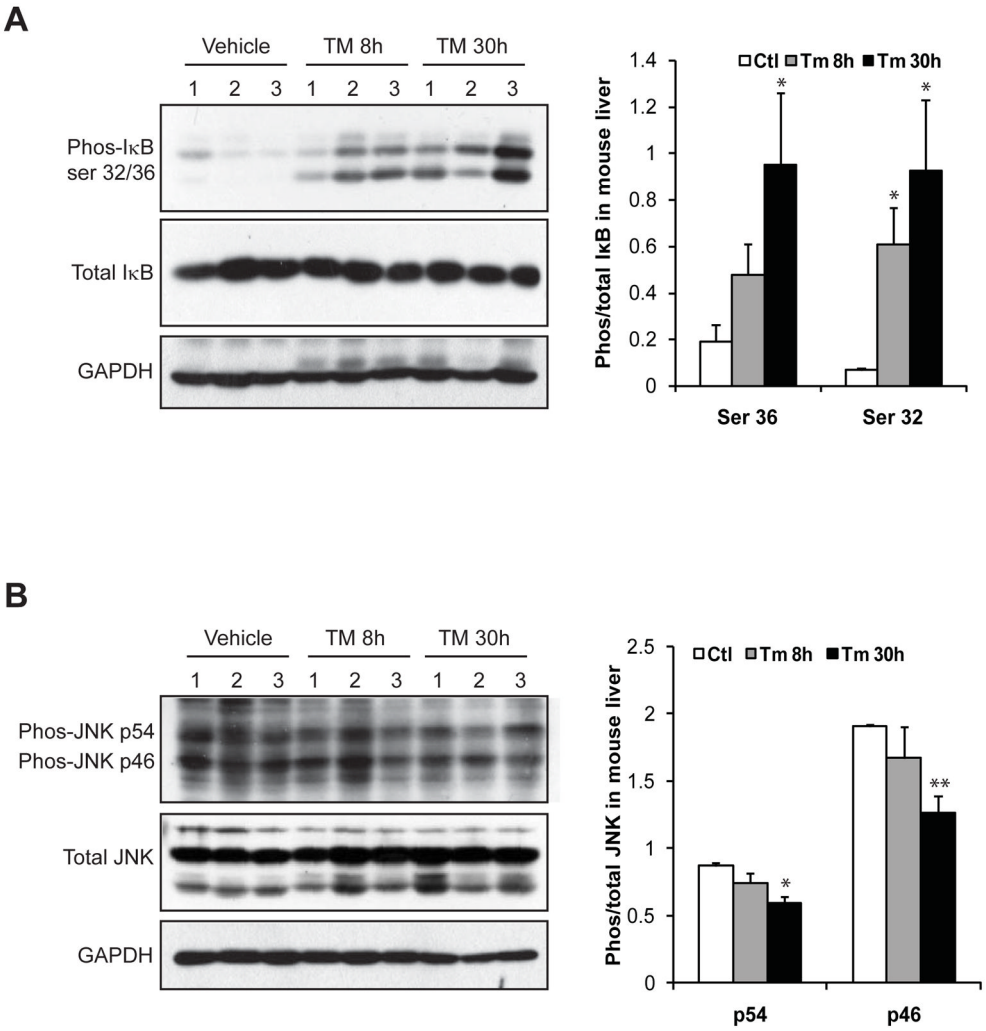

Figure 5. TM activates the inflammatory pathway through NF-κB, but not JNK, in the liver

Western blot analysis of phosphorylated Iκ-B, total Iκ-B, phosphorylated JNK, and total JNK in the liver tissues from the mice challenged with TM (2 μg/gram body weight) or vehicle control. Levels of GAPDH were included as internal controls. The graphs beside the images show the ratios of phosphorylated IkB or JNK to total IkB or JNK protein signal intensities. Each bar represents the mean ± SEM (n=3 mice per group);* $P<0.05$, ** $P<0.01$.

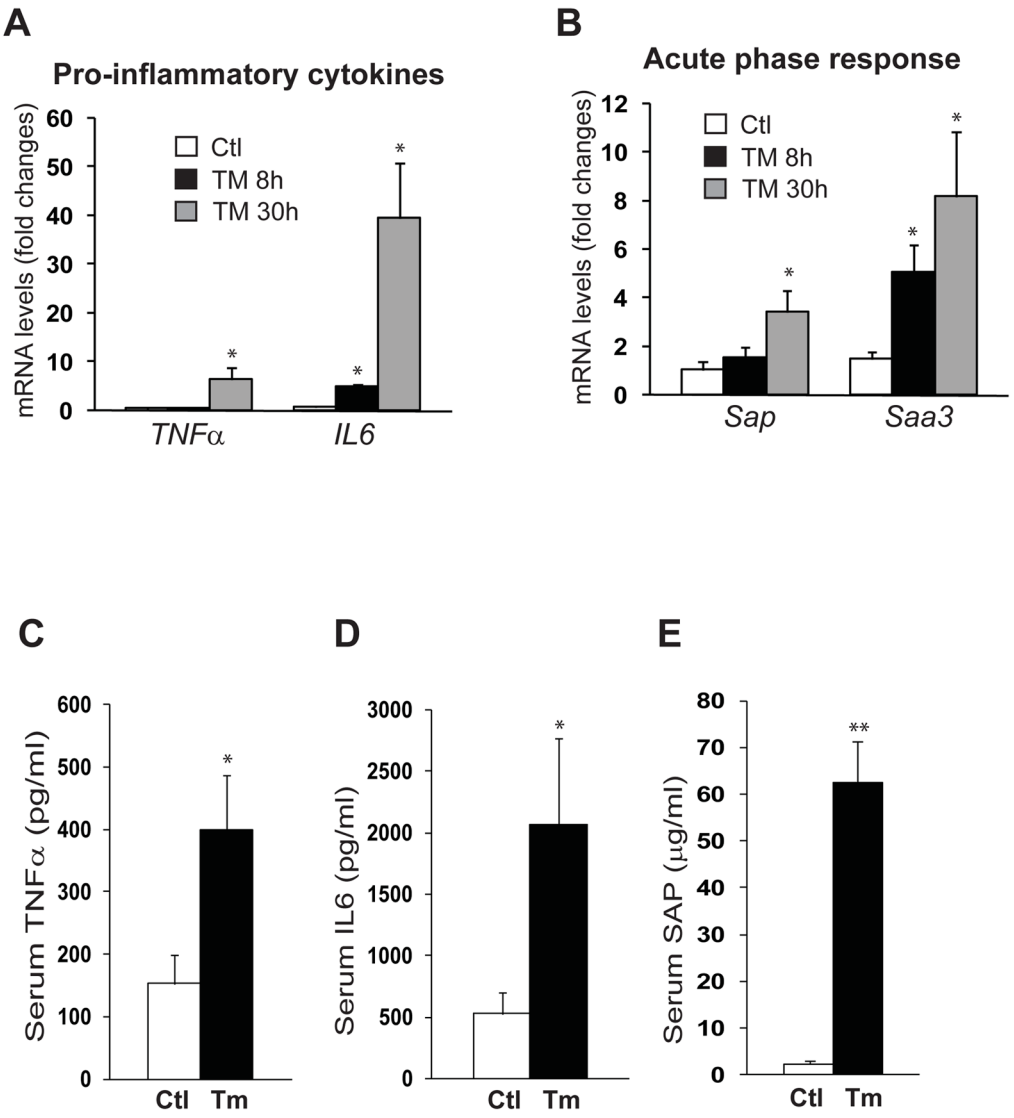

Figure 6. TM induces expression of pro-inflammatory cytokines and acute-phase responsive proteins in the liver

Quantitative real-time RT-PCR analyses of liver mRNAs isolated from the mice challenged with TM (2 μg/gram body weight) or vehicle control, which encode: (A) pro-inflammatory cytokine TNFα and IL6; and (B) acute-phase protein SAP and SAA3. Expression values were normalized to *β-actin* mRNA levels. Fold changes of mRNA are shown by comparing to one of the control mice. (C-E) ELISA analyses of serum levels of TNFα, IL6, and SAP in the mice challenged with TM or vehicle control for 8 hours ELISA. Each bar denotes the mean ± SEM (n=4 mice per group); * $P<0.05$, ** $P<0.01$.